A NUMERICAL STUDY OF NEAR CLOUD TURBULENCE ENCOUNTERS OVER BANGKA ISLAND ON 4 MAY 2016

Bayu Retna Tri Andari[1,2*], Nurjanna Joko Trilaksono[2,3] and Muhammad Arif Munandar[4]
[1]Master Program in Earth Science, Faculty of Earth Sciences and Technology, Institut Teknologi Bandung, Ganesa Street, Bandung, 40132
[2]Weather and Climate Prediction Laboratory, Faculty of Earth Sciences and Technology, Institut Teknologi Bandung, Ganesa Street, Bandung, 40132
[3]Atmospheric Science Research Group, Faculty of Earth Science and Technology, Institut Teknologi Bandung, Ganesa street, Bandung, 40132
[4]Aviation Meteorological Center, Badan Meteorologi Klimatologi dan Geofisika, Angkasa Street, Central Jakarta, 10720
*E-mail**: andaribayu@gmail.com

Received: 8 July 2022 Revised: 27 July 2022 Accepted: 1 August 2022

ABSTRACT

Accurate weather forecasts should support the increase in safety of aviation operations in Indonesia. This weather forecast is needed, especially in detecting turbulence, considering that geographically Indonesia has effective solar radiation resulting in convective cloud formation. Convective clouds can trigger turbulence and then produce disruption and even accidents on flights. This research uses a case study on the Etihad Airways flight on Bangka Island which had turbulence on May 4, 2016. At the time of the incident, there was turbulence at 39,000 feet altitude, and the aircraft did not enter the cloudy area. The Weather Research and Forecasting (WRF) model is employed to simulate the turbulence in this study, which is downscaled up to 3 km with a microphysics parameterization of WRF Single Moment 6 Class (WSM6). The results were then verified using correlation and linear regression for temperature, wind direction, wind speed, and pattern resemblance between cloud fraction and the convective nuclei distribution. The turbulence is analyzed from the south-north and west-east vertical airflow. The turbulence was spotted at 06.40 UTC when there is a quite strong updraft which can cause turbulence. The turbulence parameters used, such as the eddy dissipation rate (EDR) parameter, which has a value of 0.05 $m^{\frac{2}{3}}s^{-1}$, Richardson number with a value of less than 0.25, and turbulence index (TI 1) with a maximum value of 4 x 10^{-7} s^{-2} found that turbulence was in a strong category. The turbulence that occurs in this study is identified as near cloud turbulence (NCT) event due to cloud formation observed in the west of the turbulence and intense updraft activity at the location of turbulence.

Keywords: Turbulence, Weather Research and Forecasting (WRF), WRF Single Moment 6 Class (WSM6), near cloud turbulence (NCT), convective clouds

1. Introduction

Improvement of operations aviation in Indonesia should be supported by increased flight safety. Accurate estimation of disturbances due to weather factors such as turbulence that occur in flight operations is important for a convectively active region such as Indonesia. The Indonesian region has effective solar radiation that makes convective clouds easy to form. Meanwhile in aviation, the weather is one of the aspects that has the highest accident effect [1].

Turbulence sources have been known, which include convective systems, jet streams, complex topography, fronts, mountain waves, and wind shears [2,3]. Sharman and Lane [4] mentioned several sources of turbulence. Convective turbulence occurs due to strong updrafts and downdrafts around convective clouds. Research conducted by Kim et al. [2] concluded that the cause of 11% moderate turbulence comes from convective activity. Mountain wave turbulence (MWT) occurs due to the rupture of the gravity waves, which generated by hitting mountains in stable atmospheric conditions [4]. Clear Air Turbulence (CAT) occurs because of an increase in wind shear, reducing stability in the jet stream, tropopause, and front areas [4]. Molarin and Svensson [5] state that CAT events can occur because of the jet stream associated with vertical wind shear (VWS).

Keller [6] has classified the critical threshold for turbulence, namely the critical threshold for moderate turbulence at 0.25 < Ri < 1 and strong turbulence at a value of Ri < 0.25. A study conducted by Storer et al. [7] states that turbulence index (TI 1) is a pretty good diagnostic for turbulence, reaching 75% of CAT

incidence. The TI threshold for the moderate category is $2x10^{-7}$ s^{-2}, and the strong category is $4x10^{-7}$ s^{-2} [8]. The turbulence phenomenon allegedly occurred on an Airbus A330-200 Etihad Airways flight EY474 route Abu Dhabi - Jakarta at an altitude of about 39,000 feet over Bangka Island. The pilot stated that the aircraft did not enter a cloudy area during the turbulence event (06.40 UTC). Therefore, it was suspected that turbulence did not occur due to the influence of convective activity. Thus, the purpose of this study is to perform a detailed analysis to investigate the atmospheric conditions during the incident and the characteristics of the intensity of the turbulence that occurred on May 4, 2016. A model simulation using regional dynamical weather prediction models such as Weather Research and Forecasting (WRF) would be an appropriate approach for those purposes.

2. Data and Methods

This study uses sounding data on May 4, 2016, at the Pangkal Pinang meteorological station. Pangkal Pinang Station was chosen because it was the closest location to the turbulence scene. Furthermore, the infrared-window channel (IR1) data of Himawari-8 satellite identifies convective clouds that can cause turbulence. A numerical model of WRF version 3.9.1 with dynamic core Advanced Research WRF (ARW) is used in this study. The National Centers for Environmental Prediction (NCEP) Global Tropospheric Analyses (final analyses; FNL) data from May 3, 2016, to May 4, 2016, are used for the WRF model input. WRF-python package is used to determine the atmospheric conditions and turbulence characteristics. Furthermore, the downscaling method will be carried out until the spatial resolution reaches 3 km. Figure 1 shows the domain of computation. Domain one (two) has 9-km (3-km) horizontal grid spacing. The model output of domain one (two) is sampled every one hour (10 minutes).

The model configuration used in this numerical experiment is shown in Table 1. The experiment design is adjusted to the time and location of the event.

Figure 1. WRF domain used.

Table 1. Configuration of the numerical experiment (namelist.input file).

Namelist.input configuration	Research domain	
	Domain 1	Domain 2
X-axis grid resolution	9 km	3 km
Y-axis grid resolution	9 km	3 km
Number of west-east grids	241	91
Number of south-north grids	161	91
Microphysics Scheme	WRF Single Moment 6 class Scheme	
Long Wave Radiation Scheme	RRTM Longwave Scheme	
Short Wave Radiation Schemes	Dudhia Shortwave Scheme	
Planetary Boundary Layer Schematic	Mellor-Yamada-Janjic Scheme (MYJ)	
Cumulus Scheme	Kain-Fritsch	

The model simulation verification process is done in two steps. First, a quantitative verification is done for prognostic meteorological parameters, namely the wind, wind speed, and temperature employing correlation and linear regression methods. The second step is qualitative verification using pattern matching of cloud fraction from the output of the WRF model and the convective nuclei of Himawari 8 satellite imagery. Convective nuclei using subtraction from the black body temperature (TBB) Himawari-8 IR1 channel value is reduced by a convective cloud threshold of 221 K, according to Yang et al. [9]. Verification of convective cloud nuclei distribution is used to determine the accuracy of the WRF model in simulating convective clouds that can cause turbulence.

Turbulence occurs in unstable atmospheric conditions. Besides that, when the wind speed and wind direction change suddenly, wind shear will occur, which can trigger turbulence. Determine the effect of vertical wind shear is viewed from several aspects. The first is seen from the spatial plot of wind direction and speed at different heights, namely at an altitude of 11.5 km and 12.25 km. Furthermore, it will be seen from the vertical plot of wind speed at an altitude of 11.5 km to 12.25 km and also the hodograph from 06.10 UTC to 07.00 UTC at that altitude. Also, it will be spatially plotted the value of vertical wind shear and static stability at an altitude of 11.5 km to 12.25 km. The cause of turbulence can also come from the convective activity that occurs. A vertical airflow plot of west-east and south-north at each altitude is used to determine the airflow that occurred on May 4, 2016, at the location of the turbulence event at an altitude of 11.5 km to 12.25 km.

Turbulence can be identified using several turbulence parameters, namely turbulent kinetic energy, which can be calculated using the eddy dissipation rate, Richardson number, and turbulence index 1. Richardson number is calculated using equation (1)

$$Ri = \frac{N^2}{\left(\frac{\partial V}{\partial z}\right)^2} = \frac{\left(\frac{g}{\theta}\right)\left(\frac{\partial \theta}{\partial z}\right)}{\left(\frac{\partial V}{\partial z}\right)^2} \quad (1)$$

while the turbulence kinetic energy is calculated using equation (2)

$$e = \frac{1}{2}\left(\overline{u^2} + \overline{v^2} + \overline{w^2}\right) \quad (2)$$

and the turbulence index 1 is calculated using equation (3)

$$TI1 = DEF \cdot VWS \quad (3)$$

According to Sharman et al. [10], the intensity of turbulence can be categorized through EDR values of $0.01\, m^{\frac{2}{3}} s^{-1}$ for weak turbulence, $0.22\, m^{\frac{2}{3}} s^{-1}$ for moderate turbulence, and $0.46\, m^{\frac{2}{3}} s^{-1}$ for strong turbulence. While the threshold for the value of Ri in this study refers to research conducted by Keller [6], and the turbulence parameter, which is TI 1 refers to the research of Ellrod and Knapp [8].

3. Results and Discussion

Convective cloud identification using the Himawari-8 Satellite. Identifying convective clouds that can cause turbulence begins by observing the presence of convective nuclei in the study area.

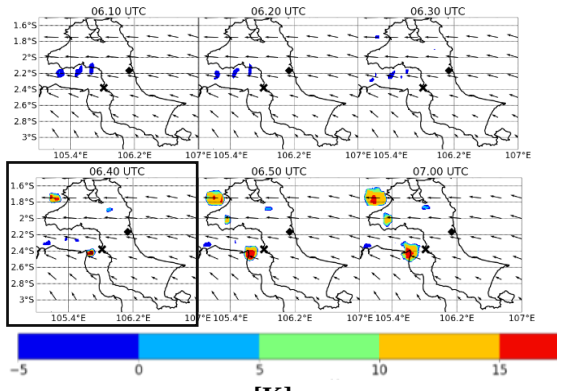

Figure 2. Convective nuclei spatial distribution from IR1 channel Himawari-8 satellite data from 06.10 UTC to 07.00 UTC, the arrow is the wind vector from FNL 06.00 UTC data, the cross symbol is the location of turbulence events, and the rhombus is the location of the Pangkal Pinang meteorological station.

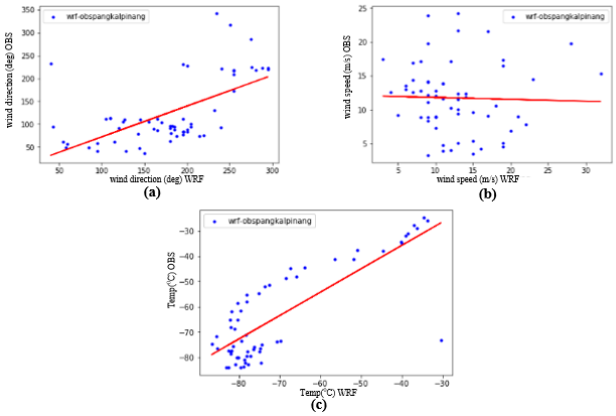

Figure 3. Scatter-plot of WRF model results with sounding data at the Pangkal Pinang meteorological station on May 4, 2016, with (a) wind direction (degree), (b) wind speed (m s^{-1}), and (c) temperature (°C).

Figure 2 shows the convective nuclei plot in the study area. From 06.10 UTC to 06.30 UTC around the study area, the convective nuclei did not appear, while at 06.40 UTC, the convective nuclei began to appear in the study area and were getting bigger until 07.00 UTC. Convective cloud growth is heading northwest as shown in Figure 2 at 06.40 UTC to 07.00 UTC to the west of the turbulence event location according to the wind direction from the initial FNL data at 06.00 UTC at an altitude of 15 mb heading northwest. Convective clouds that are growing can cause turbulence. Convective turbulence can be associated with activity outside the convective cloud, which is called near cloud turbulence (NCT), following the result from Sharman and Lane [4]. To confirm the source of turbulence, a numerical experiment is performed.

WRF Model Verification. Figure 3 shows a scatterplot and linear regression of the WRF model results with Pangkal Pinang station sounding data on May 4, 2016, at 00.00 UTC and 12.00 UTC with wind direction, wind speed, and temperature variables. The linear regression results show that the wind direction and temperature parameters have positive linear regression, but the wind speed parameters have negative linear regression.

The correlation value between the WRF model results and the observation station data obtained the correlation value in the wind direction parameter on May 4, 2016, has a value of 0.6 while the wind speed parameter is -0.03 and the temperature parameter has a correlation value of 0.81.

The existence of a convective cloud can be one of the causes of turbulence, so it is necessary to look at the accuracy of the output of the WRF model in describing the cloud distribution pattern in turbulence

events using cloud fraction variables. Figure 4 shows cloud fraction and convective nuclei distribution from the Himawari-8 satellite image at 06.30 UTC, 06.40 UTC, and 06.50 UTC. 06.30 UTC, 06.40 UTC, and 06.50 UTC were chosen because it takes time before the turbulence event, during the turbulence event, and after the turbulence event to get a representative result.

The cloud fraction output variable from the WRF model shows that the cloud area is larger and wider than the cloud area from the convective nuclei. However, in general, the cloud fraction and convective nuclei variables have the same pattern between the output of the WRF model and the Himawari-8 satellite image data around the turbulence location, which is marked off with a black circle.

Quantitative verification uses wind direction and wind speed parameters show a positive linear regression and a pretty good correlation. While qualitative verification using pattern match between cloud fraction and convective nuclei distribution has the same pattern match, the WRF model can simulate turbulence at the time and area of study.

Atmospheric conditions during the Turbulence Incident. Etihad Airways aircraft had turbulence on May 4, 2016, at an altitude of 39000 feet (11.75 km). Figures 5 (a) and (b) represent wind direction at 06.30 UTC and 06.40 UTC at an altitude of 11.5 km and 12 km. The wind moving at an altitude of 11.5 km indicated by the green vector moves eastward at 06.30 UTC, while the wind direction at an altitude of 12 km indicated by the black vector moves to the northwest. At 06.30 UTC, at an altitude of 11.5 km and 12 km, there is a difference in wind speed of 4 $m\,s^{-1}$. Meanwhile, at 06.40 UTC, the wind direction shown at an altitude of 11.5 km and 12 km does not show a difference in wind direction with a speed difference of 4 $m\,s^{-1}$. The difference in wind speed shows wind shear vertically but without changes in wind direction between altitudes at 06.40 UTC in the study area.

When viewed from the value of the vertical profile of wind speed, at 06.10 UTC to 07.00 UTC at an altitude of 11.5 km to 12.25 km, there is a pretty small difference in speed as shown in Figure 6. Meanwhile, when viewed the hodograph at 06.10 UTC to 07.00 UTC at the location of the turbulence event shows the direction of the wind moving northwest and does not change with increasing time from 0610 UTC to 07.00 UTC as shown in Figure 7.

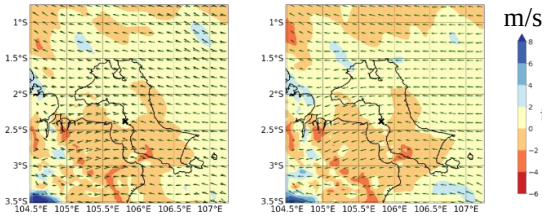

Figure 5. The plot of wind direction at 11.5 km (green vector) and 12.25 km (black vector) and wind speed (shaded) at a) 06.30 UTC and b) 06.40 UTC with a cross are the locations of turbulence events.

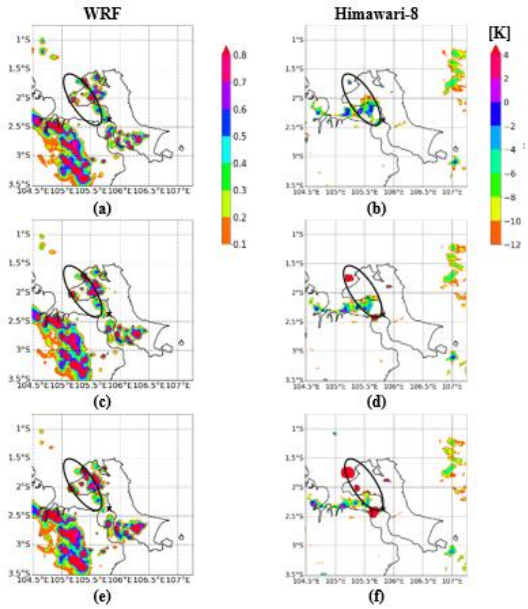

Figure 4. Convective nuclei distribution plot at (a) and (b) 06.30 UTC, (c) and (d) 06.40 UTC, and (e) and (f) 06.50 UTC with a cross are the locations of turbulence events.

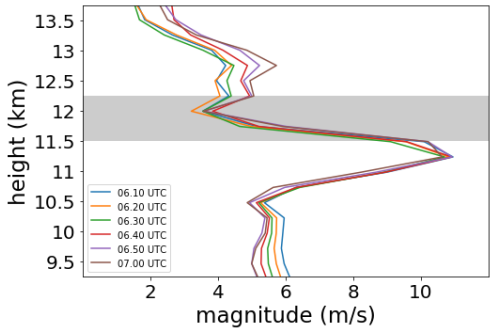

Figure 6. Plot of wind speed on May 4, 2016, vertical to the altitude of 06.40 UTC at the turbulence event location (2.375°S and 105.812°E) with a gray rectangle representing the height of the aircraft when experiencing turbulence.

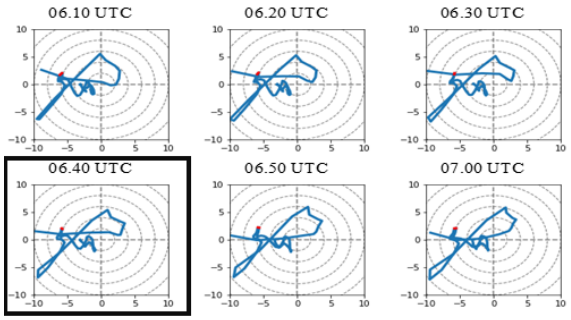

Figure 7. Hodograph plot on May 4, 2016, at 06.10 UTC to 07.00 UTC at the turbulence scene (2.375°S and 105.812°E), the black box represents the time of turbulence, and a red sign indicates the altitude of the aircraft when it experiences turbulence.

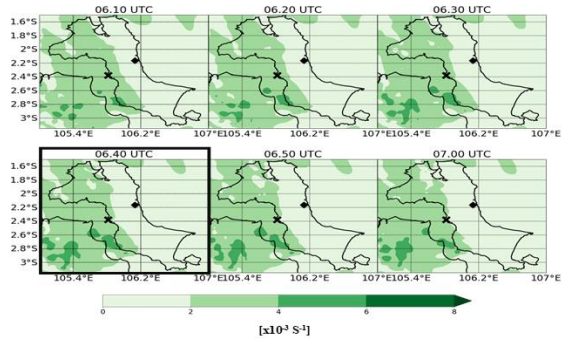

Figure 8. Plot of vertical wind shear at 06.10 UTC to 07.00 UTC at an altitude of 11.5 km to 12.25 km with the black box representing the time of turbulence and the cross is the location of the turbulence event and the rhombus sign is the location of the Pangkal Pinang meteorological station.

Vertical wind shear can trigger turbulence. Figure 8 shows the vertical wind shear (VWS) value at an altitude of 11.5 km to 12.25 km in the study area from 06.10 UTC to 07.00 UTC with turbulence occurring at 06.40 UTC, which is marked with a black box. The VWS value at the location of the turbulence event marked with a cross has a VWS value of 4×10^{-3} s^{-1} from 06.10 UTC to 07.00 UTC.

Figure 9 shows vertical airflow of south-north in the study area before to after the turbulence, which is from 06.10 UTC to 07.00 UTC with a dotted line representing the location of the turbulence event with the black box representing the altitude of the aircraft when experiencing turbulence, which is at 11.5 km to 12.25 km. Before the turbulence occurred, namely at 06.10 UTC, the vertical airflow at the scene experienced an updraft with a maximum speed of 0.2 m s^{-1}accompanied by a downdraft airflow at an altitude before 10.5 km, while at 06.20 UTC, at the scene of an updraft from an altitude of 6.5 km with a

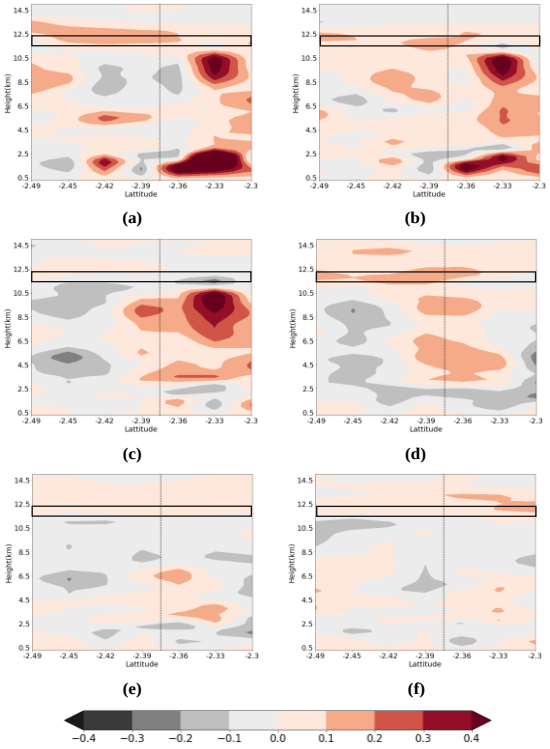

Figure 9. Plot of south-north vertical airflow against altitude at 4 May 2016 at (a) 06.10 UTC, (b) 06.20 UTC, (c) 06.30 UTC, (d) 06.40 UTC, (e) 06.50 UTC, and (f) 07.00 UTC with the dashed line is the location where turbulence occurs (2.375°S) and the black mark is the altitude of the aircraft when experiencing turbulence.

maximum speed of 0.2 m s^{-1} and 06.30 UTC, the vertical airflow experienced a downdraft at an altitude of 11.5 km to 12.25 km. Meanwhile, when turbulence occurs, at 06.40 UTC, the value of vertical airflow shows the updraft has a significant increase, with a maximum speed of 0.2 m s^{-1} from an altitude of 3 km to 14.5 km. After turbulence at 06.50 UTC and 07.00 UTC, the vertical airflow has decreased in the updraft value reaching a maximum speed of 0.1 m s^{-1} and is accompanied by a downdraft below an altitude of 11.75 km.

Figure 10 shows vertical airflow of west-east at the location of the turbulence event, which is shown by a dotted line before to after the turbulence, which is from 06.10 UTC to 07.00 UTC, with the black box representing the height of the turbulence at 11.5 km up to 12.25 km. Before the turbulence occurred, namely at 06.10 UTC, the vertical airflow at the scene experienced updraft with a maximum speed of 0.1 m s^{-1} in the presence of downdraft airflow at an altitude between 5 km to 10.5 km. While at 06.20 UTC, the scene is experiencing an updraft from an altitude of 6.5 km to 12.5 km. At 06.30 UTC, the vertical airflow experienced a downdraft at an altitude

of 10.5 km to 14.5 km. Meanwhile, when turbulence occurs, namely at 06.40 UTC, the value of vertical airflow shows the updraft has a significant increase, namely with a maximum speed of 0.2 m s^{-1} from an altitude of 3 km to 14.5 km.

After turbulence at 06.50 UTC, the vertical airflow experienced a downdraft at the altitude of 11.5 km to 12.25 km, and at 07.00 UTC, the vertical airflow experienced updraft at the altitude of 11.5 km to 12.25 km and was accompanied by a downdraft at an altitude before 11.5 km. This is consistent with the study conducted by Lane et al. [3], which states that turbulence can occur due to the influence of a strong updraft.

Sharman and Lane [4] state that when $N^2 < 0$ or $\frac{\partial \theta}{\partial z} < 0$, the static stability value is positive, and the atmosphere will experience an unstable condition. Figure 11 shows the static stability value at 06.10 UTC to 07.00 UTC at the altitude of 11.5 km to 12.25 km. In the study area, the turbulence event marked with a cross and the time of turbulence marked with a black box has a static stability value between 5.05 × 10^4 KPa^{-1} to 5.06 × 10^4 KPa^{-1}. It indicates that at an altitude of 11.5 km to 12.25 km, the atmosphere is unstable.

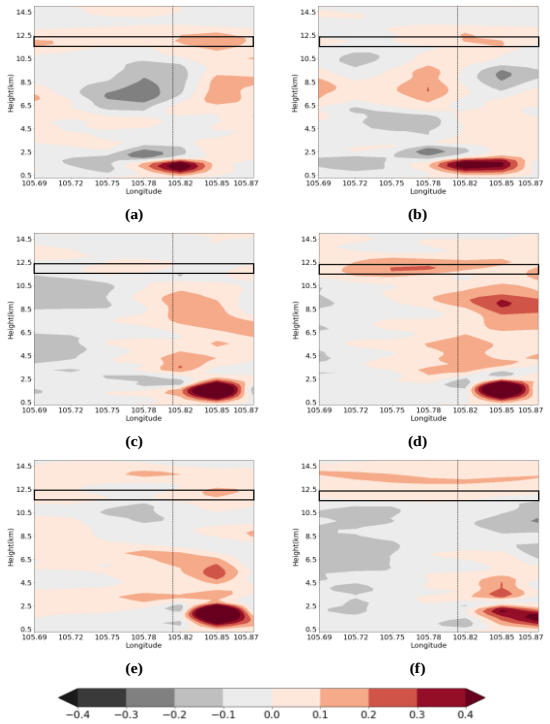

Figure 10. Plot of west-east vertical airflow versus altitude at (a) 06.10 UTC, (b) 06.20 UTC, (c) 06.30 UTC, (d) 06.40 UTC, (e) 06.50 UTC, and (f) 07.00 UTC with dashed line is the location of turbulence (105.812°E) and the black mark is the altitude of the aircraft when experiencing turbulence.

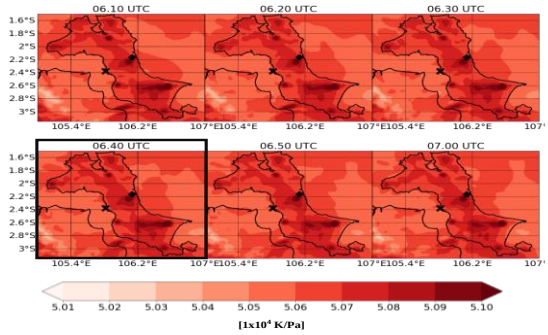

Figure 11. Static stability plot on 4 May 2016 at 06.00 UTC to 07.00 UTC at an altitude of 11.5 km to 12.25 km with a black box showing the time of turbulence and across is the location of turbulence events and a rhombus is the location of the Pangkal Pinang meteorological station.

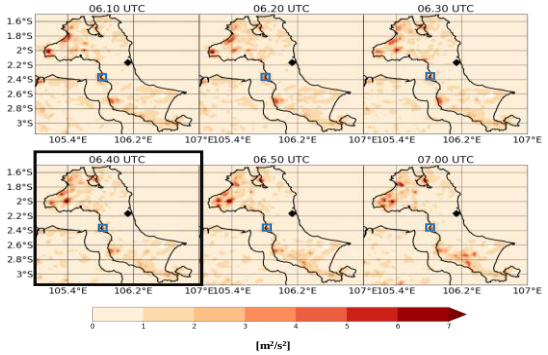

Figure 12. Turbulent kinetic energy on May 4, 2016, from 06.10 UTC to 07.00 UTC at an altitude of 11.5 km to 12.25 km with a black box showing the time of turbulence and a black box representing the location of the turbulence event and a rhombus sign is the location of the Pangkal Pinang meteorological station.

Quantification of Turbulence Intensity Parameters. Based on research conducted by Trier et al. [11], turbulent kinetic energy (TKE) can be used to calculate EDR. Figure 12 shows the turbulent kinetic energy value at 06.10 UTC to 07.00 UTC at an altitude of 11.5 km to 12.25 km. The TKE value at the location of the incident has a value of 4 m^2 s^{-2} while at the time of the turbulence, which is 06.40 UTC marked with a black box, has a TKE value of 5 m^2 s^{-2}. If calculated roughly using the assumption Δ 180 m, then at 06.40 UTC, it has an EDR value of 0.05 $m^{\frac{2}{3}} s^{-1}$.

Research conducted by Sharman et al. [10] states that the EDR value for strong turbulence is 0.046 $m^{\frac{2}{3}} s^{-1}$, using this threshold value, at 06.40 UTC at the location of the incident experienced strong turbulence.

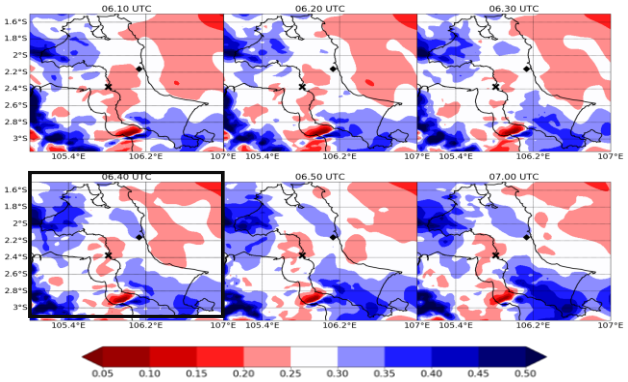

Figure 13. Spatial plot of Richardson number on May 4, 2016, from 06.10 UTC to 07.00 UTC at an altitude of 11.5 km to 12.25 km with a black box showing the time of turbulence and the cross is the location of the turbulence event, and the rhombus is the location of the Pangkal Pinang meteorological station.

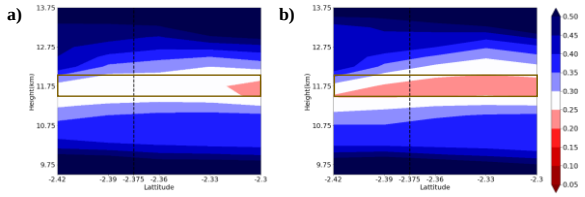

Figure 14. The vertical plot of Richardson number on May 4, 2016, at (a) 06.30UTC and (b) 06.40UTC with the dotted line is the location of turbulence, and the brown box shows the height of the aircraft when experiencing turbulence.

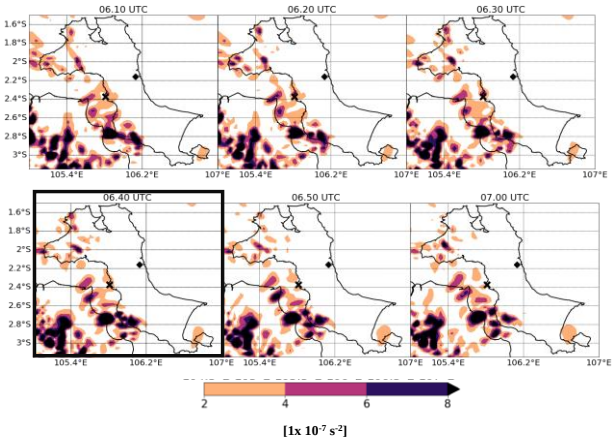

Figure 15. Plot of TI 1 on May 4, 2016, from 06.10 UTC to 07.00 UTC at an altitude of 11.5 km to 12.25 km with a black box showing the time of turbulence and the cross is the location of turbulence events and the rhombus is the location of the Pangkal Pinang meteorological station.

The spatial Richardson number is shown in Figure 13. The Richardson number at 06.10 UTC and 07.00 UTC in the study area varies considerably between 0.05 and 0.50. Before the turbulence event, at 06.10 UTC to 06.30 UTC at the location of the turbulence event marked with a cross has a Ri value ranging from 0.25 to 0.30. However, during and after the turbulence event at 06.40 to 07.00 UTC at the location of the incident it has a Ri value with a range from 0.20 up to 0.25.

Based on research by Ellrod and Knapp [8], when the Ri value is between 0 <Ri <0.25, KHI can be formed. Using the turbulence threshold classification from Keller [6], strong turbulence occurs at 06.40 UTC, indicated by the Ri value of less than 0.25. The vertical section of Richardson number is shown in Figure 14. At the location of the turbulence at the altitude of 11.5 km to 12.25 km (indicated by a brown box) at 06.30 UTC, the Ri value is more than 0.25. While at 06.40 UTC, the Ri value is less than 0.25 indicated strong turbulence.

The horizontal section of the TI1 turbulence index calculation results on May 4, 2016, from 06.10 UTC to 07.00 UTC, is shown in Figure 15. The TI1 index value in the study area is in the range of 2×10^{-7} s^{-2} to 8×10^{-7} s^{-2}. The TI 1 index value at the turbulence location, which is marked off with a cross, before the turbulence event at 06.10 UTC, 06.20 UTC, and 06.30 UTC, shows a maximum value of 6×10^{-7} s^{-2}. While at the time of the turbulence event it is marked with a black box, namely at 06.40 UTC, the TI index value at the location of the incident shows a maximum value of 4×10^{-7} s^{-2}, and after the turbulence event at 06.50 UTC and 07.00 UTC, the TI index value is less than 2×10^{-7} s^{-2}. Based on the TI 1 threshold from the research of [8], at 06.40 UTC using the NMC-AVN model, there was strong turbulence at the scene.

4. Conclusion

A numerical experiment has been conducted to investigate aviation turbulence encountered by Etihad Airways aircraft on May 4, 2016, over Bangka Island. Based on the results of research obtained that the turbulence on Etihad Airways aircraft is a near cloud turbulence (NCT) event due to cloud growth to the west of the incident site and high updraft activity at the turbulence scene. The model simulation also found that turbulence was in a strong category using the EDR parameter with a value of 0.05 $m^{\frac{2}{3}} s^{-1}$, Richardson number with a value of less than 0.25, and TI 1 with a maximum value of 4. $\times 10^{-7}$ s^{-2}. The detail of turbulence structure both spatial and temporal is shown to be relatively satisfying, which indicates that the current model configuration can capture the evolution of turbulence.

The present study mainly aims to examine the ability of the numerical weather prediction model in simulating aviation turbulence. A similar study can be

performed to examine other aircraft incidents to find out the source of turbulence. Another aspect that should be considered is the choice of vertical coordinate, which determines the location of turbulence. Hybrid vertical coordinate in the WRF model is another thing that should be explored.

Acknowledgments

We thank Institut Teknologi Bandung for supporting our research through Research and Innovation Program (P3MI) 2020.

References

[1] Eick D 2013 Turbulence Related Accidents & Incidents *Natl. Transp. Saf. Board*

[2] Kim J H, Chun H Y, Sharman R D and Keller T L 2011 Evaluations of Upper-Level Turbulence Diagnostics Performance Using the Graphical Turbulence Guidance (GTG) System and Pilot Reports (PIREPs) over East Asia *J. Appl. Meteorol. Climatol.* 1936–52

[3] Lane T P, Sharman R D, Trier S B, Fovell R G and Williams J K 2012 Recent advances in the understanding of near-cloud turbulence *Bull. Am. Meteorol. Soc.* **93** 499–515

[4] Sharman R and Lane T 2016 *Aviation Turbulence: Process , Detection, Prediction*

[5] Molarin K and Svensson G 2013 Case study of CAT over the North Atlantic Ocean

[6] Keller J L 1981 Prediction and Monitoring of Clear-Air Turbulence: an Evaluation of the Applicability of the Rawinsonde System. *J. Appl. Meteorol.* **20** 686–92

[7] Storer L N, Williams P D and Gill P G 2019 Aviation Turbulence: Dynamics, Forecasting, and Response to Climate Change *Pure Appl. Geophys.* **176** 2081–95

[8] Ellrod G P and Knapp D I 1992 An Objective Clear-Air Turbulence Forecasting Technique: Verification and Operational Use *Weather Forecast.* **7** 150–65

[9] Yang X, Fei J, Huang X, Cheng X, Carvalho L M V and He H 2015 Characteristics of mesoscale convective systems over China and its vicinity using geostationary satellite FY2 *J. Clim.* **28** 4890–907

[10] Sharman R D, B.Cornman L, G.Meymaris, Pearson J and Farrar T 2014 Description and Derived Climatologies of Automated In Situ Eddy-Dissipation-Rate Reports of Atmospheric Turbulence *J. Appl. Meteorol. Climatol.* 1416–32

[11] Trier S B, Sharman R D dan Lane T P 2012 Influences of Moist Convection on a Cold-Season Outbreak of Clear-Air Turbulence (CAT) *Mon. Weather Rev.* 2477–97.